Journal of Earth Science, *Vol. 27*, *No. 4*, *p. 584–598*, *August 2016* *ISSN 1674-487X*
Printed in China
DOI: 10.1007/s12583-016-0717-1

Interrelationships between Deformation and Metamorphic Events across the Western Hinterland Zone, NW Pakistan

Asghar Ali*[1], Mustafa Yar[2], Muhammad Asif Khan[3], Shah Faisal[3, 4]
1. *Department of Geology*, *University of Peshawar*, *Khyber Pakhtunkhwa* 25120, *Pakistan*
2. *Department of Earth and Environmental Sciences*, *Bahria University*, *Islamabad* 44000, *Pakistan*
3. *National Centre of Excellence in Geology*, *University of Peshawar*, *Khyber Pakhtunkhwa* 25120, *Pakistan*
4. *Earth and Environmental Sciences*, *IKBAS*, *University of British Columbia*, *Okanagan Kelowna BC VIV* 1*V*7, *Canada*

ABSTRACT: Microscopic to mesoscopic structural investigations and foliation intersection axes (FIAs) preserved in porphyroblasts reveal a very complex history of deformation and tectonism within the southwestern part of the western hinterland zone along the northern margin of the Indian plate, NW Pakistan. D_1, D_2, and D_3 related structures in the southwestern part resemble the F_1/F_2, F_3, and F_4 related structures in the northeastern part of the western hinterland zone. These structures developed at the same time through the same changes in the direction of bulk shortening in southwestern and northeastern parts of the western hinterland zone. FIA set 1 indicates NW-SE shortening. The D_2 fabrics, mineral lineations and fold axes indicate E-W shortening. FIA set 2, D_3 fold axes and mineral lineations indicate NNE-SSW shortening. D_3 deformation event is equivalent to the F_4 deformation event in the northeastern part of the western hinterland zone. D_4 fold axes, mineral stretching lineations and axial plane foliation suggest ENE-WSW shortening. The D_4 NNW-SSE fabrics, which formed in the region after the formation of the MMT (main mantle thrust), Khairabad-Panjal thrust fault, Hissartang thrust fault and MBT (main boundary thrust), likely resulted from ENE-WSW bulk shortening related to development of the Hazara-Kashmir syntaxis.
KEY WORDS: FIA, western hinterland zone, microstructure, mesostructure, metamorphism, tectonics, NW Pakistan.

0 INTRODUCTION

The northern Pakistan comprises of three major tectonic blocks separated by the main boundary thrust (MBT) and the main mantle thrust (MMT, Pogue et al., 1999). Deformed sedimentary rocks of the Kohat and Potwar Sub-Himalayas are exposed to the south of the MBT and the MMT separates the Indian plate rocks from the Kohistan island arc (Fig. 1a; Treloar et al., 1992). The tectonic terrain between the MMT and MBT is characterized by the regional scale Khairabad and Panjal thrusts. The region located south of the MMT, north of Khairabad thrust and west of Panjal thrust has been called the western hinterland zone of Pakistan (DiPietro et al., 2008). The western hinterland zone records increasing grade of metamorphism and deformation from south to north (Pogue et al., 1999). The study area, which consists of multiply deformed metasedimentary rocks (Silurian–Devonian Lowara Mena Formation and Warsak metamorphic complex), crops out in the southwestern part of the western hinterland zone (Fig. 1a). According to Ahmad et al. (1969), the area consists of metasediments of green schist facies rocks (slate, phyllites, graphitic schists, mica schist, garnet schist, hornblende schist, calcareous schist and marble). The tectonic and structural relationship of the southwestern part with the northeastern part of the western hinterland zone is poorly constrained because the eastern continuation of the Khyber stratigraphic sequence is eroded and covered by younger sediments of the Peshawar Basin (Fig. 1a). The nature of the tectonic setting in the area is based currently on generalized regional geological traverses and random petrography (e.g., Khan et al., 1989; Shah et al., 1980; Ahmad et al., 1969). The southwestern part of the hinterland zone has been regionally mapped without establishing multiple deformation and metamorphic events and their correlation across the western hinterland zone.

This research uses detailed microscopic structures preserved in porphyroblasts and matrix, foliation intersection axes preserved in porphyroblasts (FIAs, Cao and Fletcher, 2012; Abu Sharib and Bell, 2011; Ali, 2010) and mesoscopic structures at outcrop scale, which provide a detailed understanding of the tectono-metamorphic evolution of the southwestern hinterland region. It establishes the interrelationship between regional scale deformation events across the western hinterland zone of Northwest Pakistan.

1 REGIONAL GEOLOGY

The Silurian–Devonian Lowara Mena Formation is exposed in the southwestern part of the western hinterland zone

*Corresponding author: asghar.ali@upesh.edu.pk

Manuscript received November 10, 2014.
Manuscript accepted December 1, 2015.

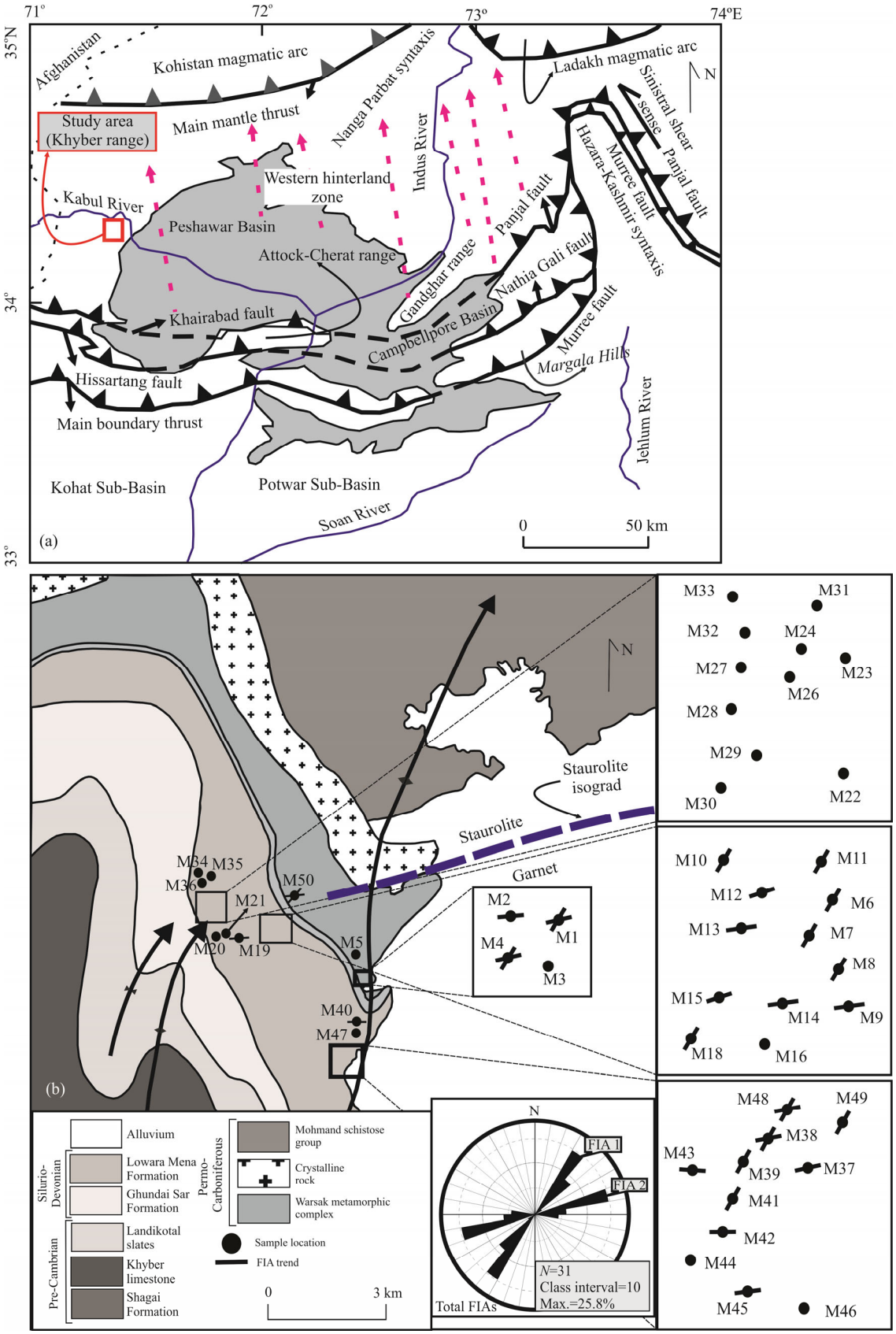

Figure 1. (a) Regional tectonic map of Pakistan showing major tectonic terrains separated by the main boundary thrust and main mantle thrust, the dashed arrows showing increase in grade of metamorphism and deformation towards north (modified after Kazmi and Rana, 1982). (b) Detailed geological map of Mula Gori area, northeastern Khyber Agency showing major stratigraphic units and sample locations (modified after Khan et al., 1989), showing the increase in grade of metamorphism from the lower amphibolite facies in the south to the middle amphibolite facies in the north, the dotted line indicates staurolite isograd, which separates the staurolite zone from the garnet zone.

of Pakistan (Fig. 1a). It predominantly consists of multiply deformed metamorphic rocks. These rocks are intruded by Permo–Carboniferous crystalline igneous rocks, which separate the Silurian–Devonian rocks of Khyber Agency from the Permo–Carboniferous rocks of the Warsak metamorphic complex and the Mohmand schistose rocks. Macroscopic scale NE-SW trending folds dominate the structural grain of the region (Fig. 1b).

DiPietro et al. (2008) established at least four deformation events in the northeastern part of the western hinterland zone through micro- to macroscopic investigations. The exposed parts of the western hinterland zone in Warsak, Nawagai, Malakand, Swat, Besham, Kaghan, Naran, Burawai, Rustam, and Swabi preserve evidence of regional scale folds F_1/F_2, F_3, and F_4 that occurred during separate tectonic events (cf., Fig. 1B of DiPietro et al., 2008). The pervasive S_2 crenulation cleavage aged ~47±3 Ma is associated with the F_1/F_2 deformation event in the western hinterland zone (see DiPietro et al., 2008 for detail). Mineral stretching lineations associated with S_2 crenulation cleavage trend variably in NE-SW and NW-SE directions. The S_2 deformation contributed to amphibolite facies metamorphism in the eastern part of the western hinterland zone. The map scale upright Eocene to Early Oligocene F_3 folds overprints both F_1/F_2 folds and crenulate the pervasive S_2 crenulation cleavage in the eastern part of the western hinterland zone. The regional scale F_3 folds trend NNE-SSW in the Nawagai region (cf., Fig. 1B of DiPietro et al., 2008). The same fold axes trend NNE-SSW in the Pinjkora anticline, Dargai, Kotah dome, Saidu, Loe Sar dome, Indus River anticline, Indus syntaxis and Hazara before bending to an NE direction near the Kohiston fault in the north (cf., Fig. 1B of DiPietro et al., 2008). The F_3 deformation event was accompanied by weak metamorphism (cf., DiPietro et al., 2008). The map scale E-W trending structures and lineations in the western hinterland zone developed during the F_4 deformation event. The E-W trending fold axes related to F_4 are nicely exposed in the Pinjkora, Swat, Malakand, Rustam, and Swabi regions (cf., Fig. 1B of DiPietro et al., 2008). These structures developed during N-S horizontal bulk shortening at ~31 to 23 Ma and thus overprinted the NNE-SSW trending structures related to F_3 across the western hinterland zone. The E-W trending regional scale Khairabad-Panjal thrust fault, Hissartang-Nathia Gali thrust fault and the MBT were then overprinted by the Hazara-Kashmir syntaxis (HKS, Fig. 1a). These E-W structures are counterclockwise rotated in the apex region of the HKS.

2 PETROGRAPHY

Fifty oriented samples were collected from the Silurio-Devonian Lowara Mena Formation. A total of 385 vertical thin sections were made from these samples with different strikes for FIA measurements (see below), petrographic and microstructural observations. Mesoscopic structures including fold axes, lineations and axial plane orientations were measured in the field. The relationship between the micro- and mesoscopic structures was established to decode the deformation events in the area.

Mineral assemblages in the metapelitic rocks consist of quartz, graphite, ilmenite, chlorite, chloritoid, biotite, muscovite, garnet, staurolite and pyrite.

2.1 Garnet

Idiomorphic, subidiomorphic and xenomorphic garnet porphyroblasts enclose inclusions of quartz, ilmenite, muscovite and biotite. The size of these porphyroblasts ranges from 0.5 to 2.5 mm. Inclusion trails preserved within them are either continuous with or truncated by the matrix foliations (Figs. 2a, 2b). Some garnet porphyroblasts exhibit changes in inclusion trail asymmetry from core to rim (Fig. 2c). In places, garnet cores with abundant inclusions and inclusion less rims were also observed. Cleavages dominated by mica are intensified and deflected around the garnet porphyroblasts. In graphitic rich layer some garnets show textural/sector zoning (Fig. 2d). Sigmoidal or very rarely spiral inclusion trails preserved in garnet porphyroblasts are much finer grained than similar grains in the matrix.

2.2 Staurolite

Staurolite porphyroblasts contain inclusions of quartz. Staurolite porphyroblasts were studied only in three samples. The strongly developed differentiated crenulation cleavage wraps the staurolite porphyroblasts (Fig. 2e). They were not used for microstructure analyses because they are not present in all vertical thin sections around the compass.

2.3 Chlorite, Biotite and Muscovite

Chlorite occurs mostly in differentiated cleavages with some as large flakes in crenulation hinges (Fig. 2f). Biotite is mainly concentrated in differentiated crenulation cleavage seams and constitutes the dominant matrix foliation. Biotite in the form of porphyroblast was not observed in any sample. Garnet and staurolite are predominantly wrapped by strongly oriented elongated biotite in the differentiated crenulation cleavage seams. Muscovite occurs in smaller amount and is generally finer grained than biotite in all samples.

2.4 Chloritoid

Chloritoid in the form of porphyroblasts was observed in two samples (Fig. 2g). It occurs in close association with chlorite. High relief and twining makes it distinct from chlorite and plagioclase. The strongly developed differentiated crenulation cleavage in the matrix truncates the poorly preserved inclusion trails in chloritoid porphyroblasts.

3 FOLIATION INTERSECTION AXES PRESERVED IN PORPHYROBLASTS (FIA) TECHNIQUE

The FIA technique was first introduced by Hayward (1990) and since then it has been successfully used by subsequent workers for quantitative analyses of microstructures which were normally destroyed in the matrix during succeeding younger deformation events (e.g., Ali, 2010; Shah, 2009; Bell et al., 2004; Bell and Hickey, 1998). FIA measurements give ample information about paleo-bulk shortening directions, which cannot be established by other means (cf., Abu Sharib and Bell, 2011). Consistent successions of changing FIA trends directly show changes in the direction of bulk shortening with time (Bell and Sapkota, 2012; Sanislav, 2010). Initially an FIA can be established in a series of six oriented thin sections for a sample by finding the flip in the asymmetry of inclusion trails preserved in porphyroblasts

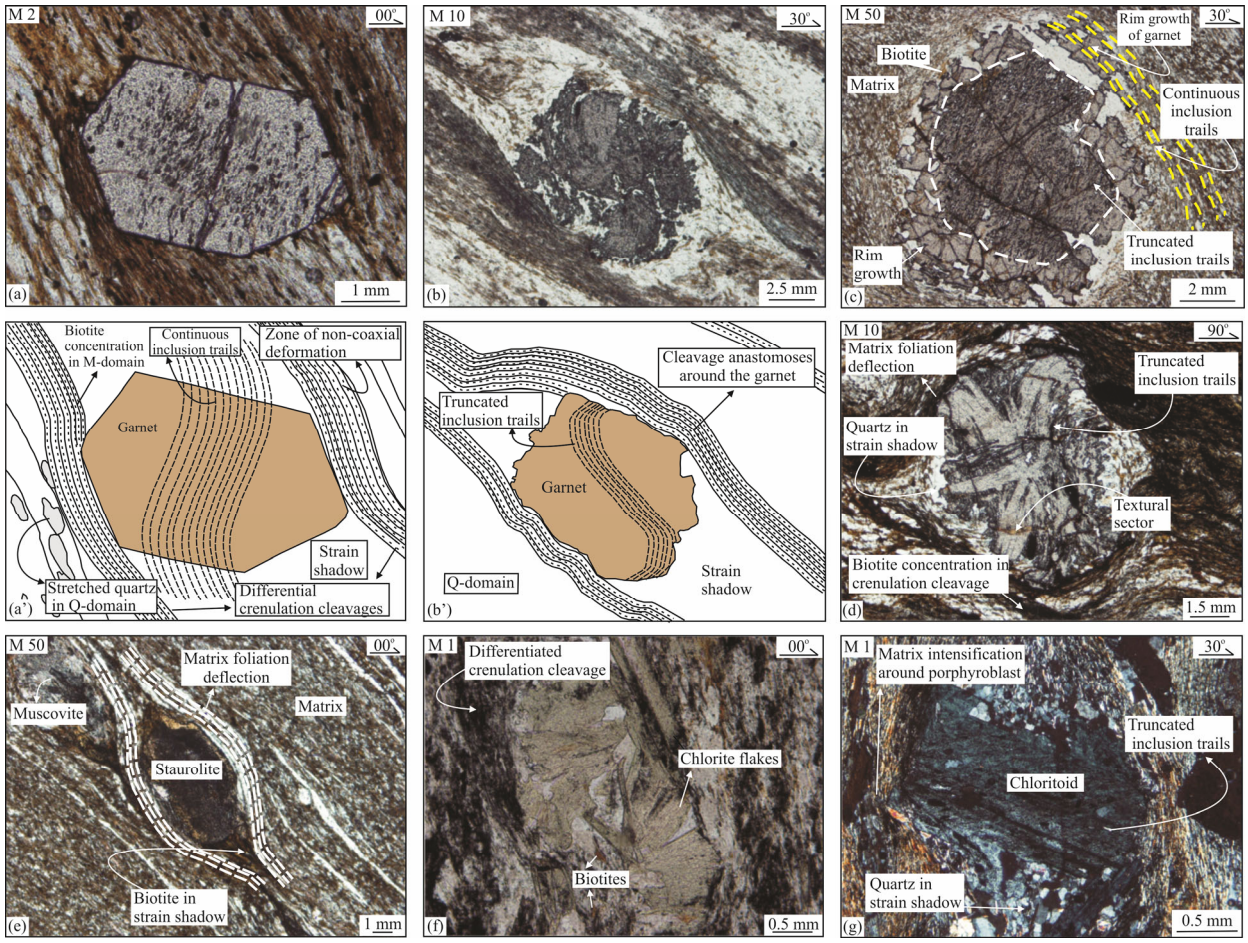

Figure 2. (a) Photomicrograph and (a') line sketch at the similar scale of a vertical thin section showing continuous inclusion trails in an idiomorphic garnet porphyroblast that are passing continuously into the matrix. (b) Photomicrograph and (b') line diagram at the identical scale from a vertical thin section showing a garnet porphyroblast with truncated inclusion trails. (c) Photomicrograph showing different asymmetries of inclusion trails in core and rim of garnet porphyroblast, the inclusion trials in the core are truncated by the inclusion trails in the rim, the inclusion trails preserved in the rim are continuous with the matrix. (d) Photomicrograph showing sector or textural zoning in garnet porphyroblast, note the matrix anastomoses around the garnet. (e) Photomicrograph illustrating elongated shaped staurolite containing fine grained S_2 foliation as inclusion trails in a zone of non-coaxially deformed matrix. (f) Photomicrograph exhibiting differentiated crenulated cleavage with chlorite flakes in microlithon in graphitic schist. (g) Photomicrograph showing inclusion trails of chloritoid porphyroblast that are truncated by the younger deformation in the matrix.

viewed in one direction around the compass (Fig. 3a). For FIA determinations, initially six vertical thin sections were cut from a horizontally oriented block at every 30° from true North. Two more vertical thin sections were cut from the same sample at 10° intervals to narrow down the FIA range between the two vertical thin sections where the asymmetries changed. The FIA trend is established as being the midway between the two oriented vertical thin sections at the 10° succession across which the flip occurs.

3.1 Foliation Intersection Axes Sets and Succession Determination

A total of 31 FIAs trending NE-SW and ENE-WSW were established within 26 samples hosting garnet porphyroblasts (Table 1; Fig. 3b). Early deformation events in multiply deformed rocks are commonly deciphered with the help of early fabrics preserved as inclusion trails in porphyroblasts of different generations (Ali, 2010). Porphyroblasts are generally more competent than the surrounding matrix and can shield early foliations/fabric from the affects of younger deformations and metamorphisms (Aerden, 2005; Cihan and Parsons, 2005). Generally foliations in the matrix obliterate or become parallel to bedding (S_0), due to reactivation and shearing (Bell et al., 2003). Consequently deformed matrix gives information only about the youngest deformation events in multiply deformed rocks (e.g., Hickey and Bell, 2001). Reactivation of pre-existing foliations in younger deformation events in the matrix obliterates important tectonic features from rocks, unless such features have not been preserved as inclusion trails in porphyroblasts (Ali, 2010; Bell, 1986). The inclusion trails within the porphyroblasts in a rock can effectively preserve differentiation asymmetries associated with crenulation cleavage development in a particular deformation event (e.g., Bell and Bruce, 2006). Porphyroblasts protecting the early differentiation asymmetries of one foliation into another in the form of inclusion trails enable to elucidate the earlier horizontal bulk shortening direction (Bell and Sapkota, 2012). Therefore preservation of differentiation asymmetries in porphyroblasts in a rock can be used for

the relative timing of folding in an orogeny where a lengthy history of deformation has been documented (Bell et al., 2003). Relative timing between different FIA sets is established on the basis of the following rules.

(1) Change in FIA trend from core to rim (Fig. 2c; Bell and Hickey, 1998).

(2) Continuity vs truncation of inclusion trails in porphyroblast by the matrix foliation (Figs. 3a, 3b, 4, and 5, Adshead-Bell and Bell, 1999).

4 FIA SETS

An equal area rose diagram of the 31 FIAs shows two dominant FIA sets with NE-SW and ENE-WSW orientations in the Mula Gori region (Fig. 3b).

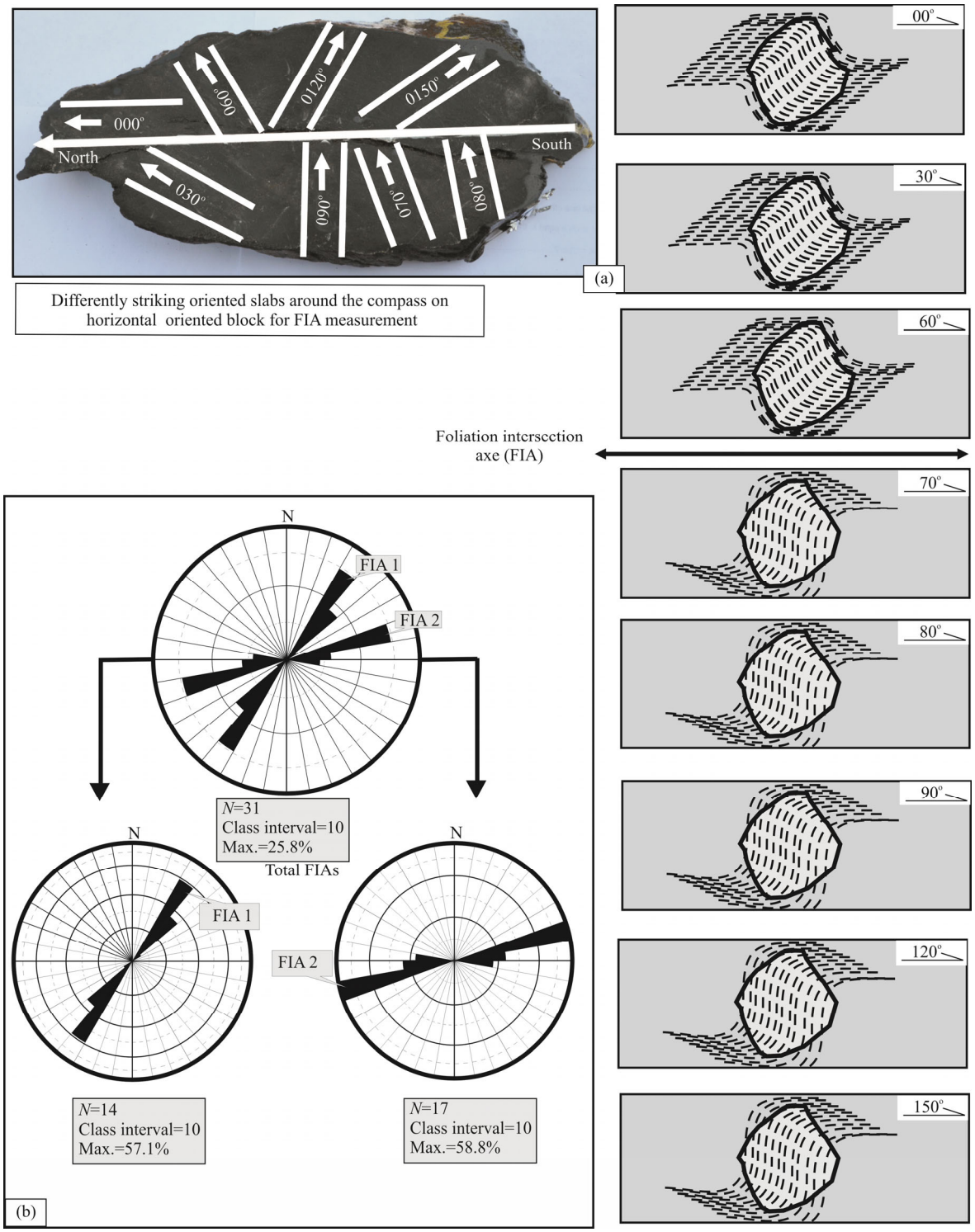

Figure 3. (a) Sketches illustrating FIA measurement technique in a series of six vertically oriented thin sections cut from a horizontal oriented block. Note the thin sections are viewed in single direction across the compass. (b) Equal area rose diagrams showing FIA sets 1 and 2 trends preserved within garnet porphyroblasts of at least two different generations.

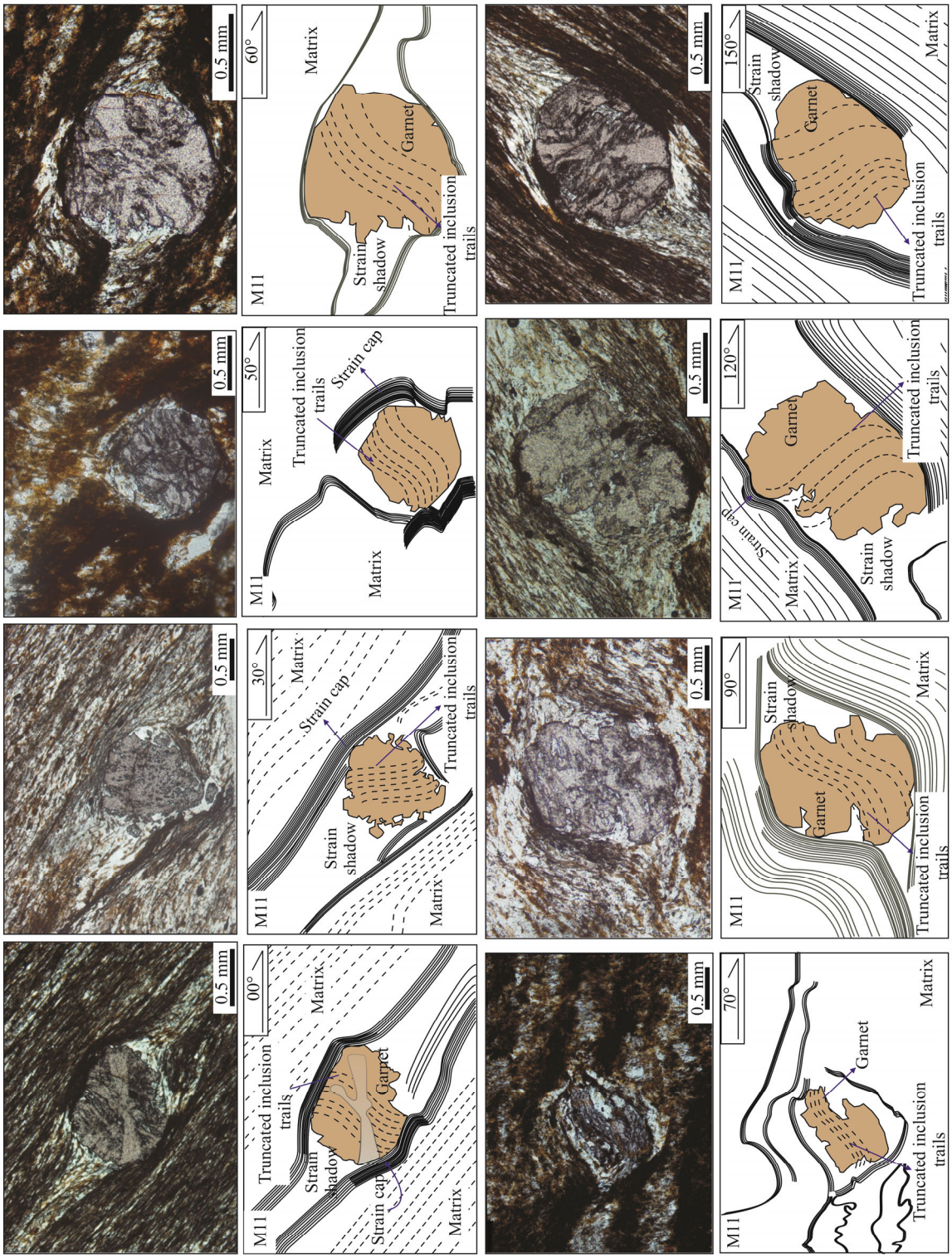

Figure 4. Oriented photomicrographs showing truncated inclusion trails with the matrix in differently oriented vertical thin section around the compass from sample M11. The inclusion trails preserved in garnet porphyroblasts are truncated by a well established crenulation cleavage in the matrix.

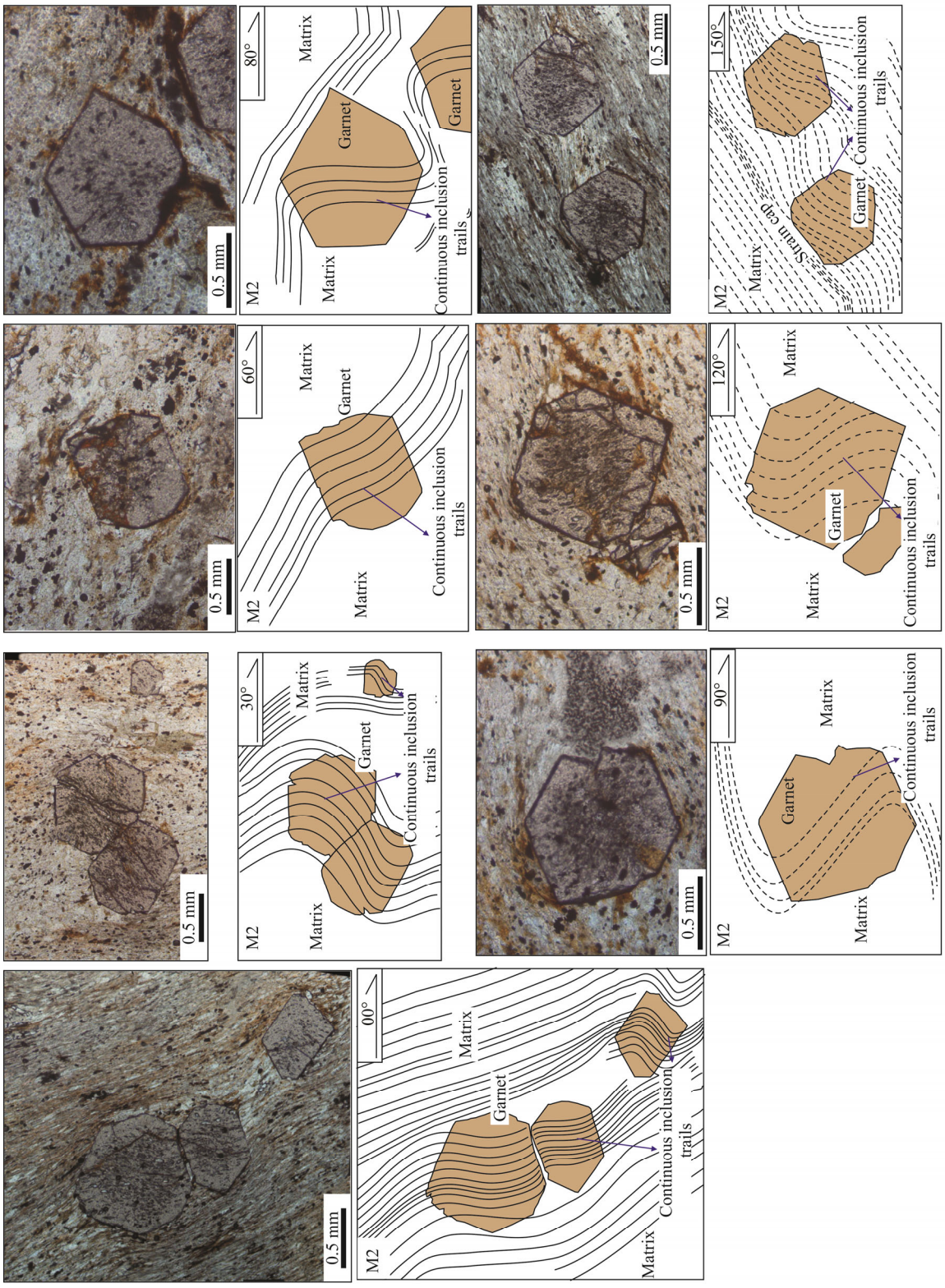

Figure 5. Oriented photomicrographs showing continuous inclusion trails with the matrix in differently oriented vertical thin sections from sample M2. Asymmetry of inclusion trails flip from counterclockwise to clockwise around vertical thin section oriented at 90°.

Table 1 Foliation intersection axis and sample locations from Mula Gori area

Samples	Easting	Northing	FIA 1	FIA 2
M1	71°22′55.4″	34°07′06.3″	40	80
M2	71°22′54.3″	34°07′06.4″	–	90
M4	71°22′54.0″	34°07′06.0″	35	70
M6	71°20′57.9″	34°08′09.0″	40	–
M7	71°20′58.6″	34°08′06.9″	35	–
M8	71°21′04.8″	34°08′04.9″	40	–
M9	71°21′06.1″	34°07′59.9″	–	90
M10	71°20′54.3″	34°08′13.8″	55	–
M11	71°20′53.1″	34°08′13.7″	35	–
M12	71°20′54.5″	34°08′08.6″	–	70
M13	71°20′52.3″	34°08′0.80″	–	85
M14	71°20′51.2″	34°08′0.08″	–	70
M15	71°20′45.4″	34°08′00.5″	–	70
M18	71°20′38.8″	34°07′54.5″	40	–
M19	71°20′12.7″	34°07′51.5″	–	70
M37	71°22′24.5″	34°05′19.9″	–	75
M38	71°22′22.1″	34°05′22.7″	35	75
M39	71°22′20.5″	34°05′22.4″	35	–
M40	71°22'.3 28″	34°05'.3 71″	–	85
M41	71°22′17.7″	34°05′21.5″	40	–
M42	71°22′15.6″	34°05′20.7″	–	90
M43	71°22′11.6″	34°05′19.9″	–	95
M45	71°22′13.5″	34°04′59.1″	–	70
M48	71°22′33″	34°05′27.6″	35	70
M49	71°22′45.4″	34°05′25.9″	35	–
M50	71°21′23.6″	34°08′20.8″	35	75

4.1 FIA Set 1

The NE-SW trending FIA set 1 was observed in the core of garnet porphyroblasts and in garnets where the inclusion trails are truncated by the matrix (Fig. 4). The inclusion trails preserved in garnets core and in garnets that predate FIA 2 are truncated by the rim inclusion trails and younger crenulation cleavages in the matrix. FIA 1 was never observed in garnets containing inclusion trails that are continuous with the matrix. FIA 1 trends average 035º–045º.

4.2 FIA Set 2

FIA set 2 was measured in the rim of the garnet porphyroblasts containing nicely developed cores plus from garnets with well developed inclusion trails that pass continuously into the matrix (Fig. 5). FIA 2 trends average 070º–085º.

5 MESOSCOPIC TO MICROSCOPIC STRUCTURES

Mesoscopic to microscopic structure investigations of the Mula Gori area show four penetrative deformation events. These events were observed in field and in oriented thin sections. The first deformation event, D_1 is preserved only as inclusion trails defining a foliation in FIA 1 garnet porphyroblasts. This event was generally obliterated in the matrix by younger superimposed deformation events. The younger deformation events that have played significant role in the tectonic evolution of the area are nicely preserved from microtomesoscopic scale. Mineral stretching and intersection lineations are well preserved across the study area.

5.1 Folds and Cleavages

Four distinct cleavages (S_1–S_4) developed during the D_1, D_2, D_3, and D_4 deformation events were recognized in these rocks. The S_1 is preserved as inclusion trails in garnet porphyroblasts. Relics of S_1 can also be seen in the Q-domains between S_2 seams in the matrix. The S_2 is the most dominant and well preserved foliation, while S_3 and S_4 were observed locally at various locations. The orientations of latter 3 foliations are plotted on the rose diagram (Fig. 6). Bedding (S_0) parallel S_2 foliations are pervasively developed in the metapelitic schist. S_3 is steeply dipping and is followed by moderately dipping S_4.

5.2 D_1/S_1

Multiple deformation commonly obliterates the remains of S_1 in tectonized terrains because of the role of reactivation of bedding and early formed foliations in deformed rocks (e.g., Bell, 1986). Thus NE-SW trending S_1 is well preserved in the form of sigmoidal inclusion trails in garnet porphyroblasts. In these rocks, the inclusion trails are predominantly defined by fine grained sigmoidal quartz (Fig. 7a).

5.3 D_2/S_2

The D_2 is a highly penetrative deformation event. This deformation event produced N-S striking upright tight folds and N-S striking S_2 axial plane penetrative crenulation cleavage. The S_2 is moderately to steeply dipping and parallel to bedding (Figs. 8a, 8b). The orientation of a cleavage in rocks is controlled by lithology (cf., Huston, 1990) and in layers accommodate folding by reactivation rather than further development of an axial plane cleavage (Bell et al., 2003; Bell, 1986). For example in interbedded pelites and psammites, the pelitic beds tend to reactivate rotating S_2 towards S_0. In the Mula Gori region, D_2 related cleavages lie parallel to bedding in the pelitic beds but when they enter into the marbleized limestone they tend to lie at a high angle to bedding (Fig. 8c; cf., Bell, 1986).

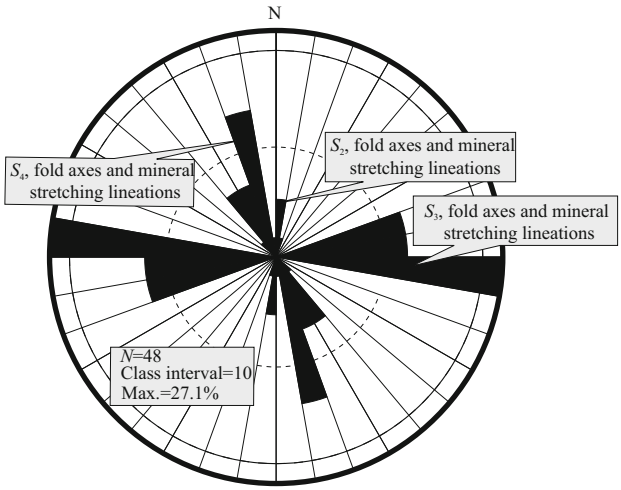

Figure 6. Equal area rose diagram showing trends of mesoscopic structures preserved in the metapelitic schist of Mula Gori area, northeastern Khyber Agency.

The penetrative S_2 cleavage, which tends to lie parallel to the bedding in the metapelites becomes the axial planes of tight folds in the marbleized and psammitic rocks in the region.

5.4 D_3/S_3

The D_3 fabrics are sub-vertical in the region. The D_3 axial plane foliations are orthogonal to S_2 foliations in the pelitic unit (Fig. 8d). The S_3 is best seen in the southern part of the Lowara Mena Formation and contains the D_3 fold axes, which are well developed in the marbleized limestone southwest of the Lowara Mena Formation (Fig. 8e). The mineral stretching lineations related to D_3 trend ENE-WSW in the pelitic unit of the formation. The S_3 is preserved both as inclusion trails in garnet porphyroblasts and in the matrix. At outcrop scale the spaced crenulation cleavages related to D_3 are predominantly defined by white mica.

5.5 D_4/S_4

The D_4 produced gently dipping S_4 foliation and crenulates penetrative S_2 in the metapsammite beds (Figs. 8f, 8g). Mesoscopic folds related to D_4 were observed locally across the Mula Gori region and are equally developed in marbleized limestone and metapsammite. The general trend of axial plane foliation related to D_4 is 340º and dips at an average of ~50º.

5.6 Lineations

Mineral lineations and fold axes are the main mesoscopic linear fabrics in the region. Mineral lineations in the plane of foliations are expressed by elongate shaped feldspar, quartz and

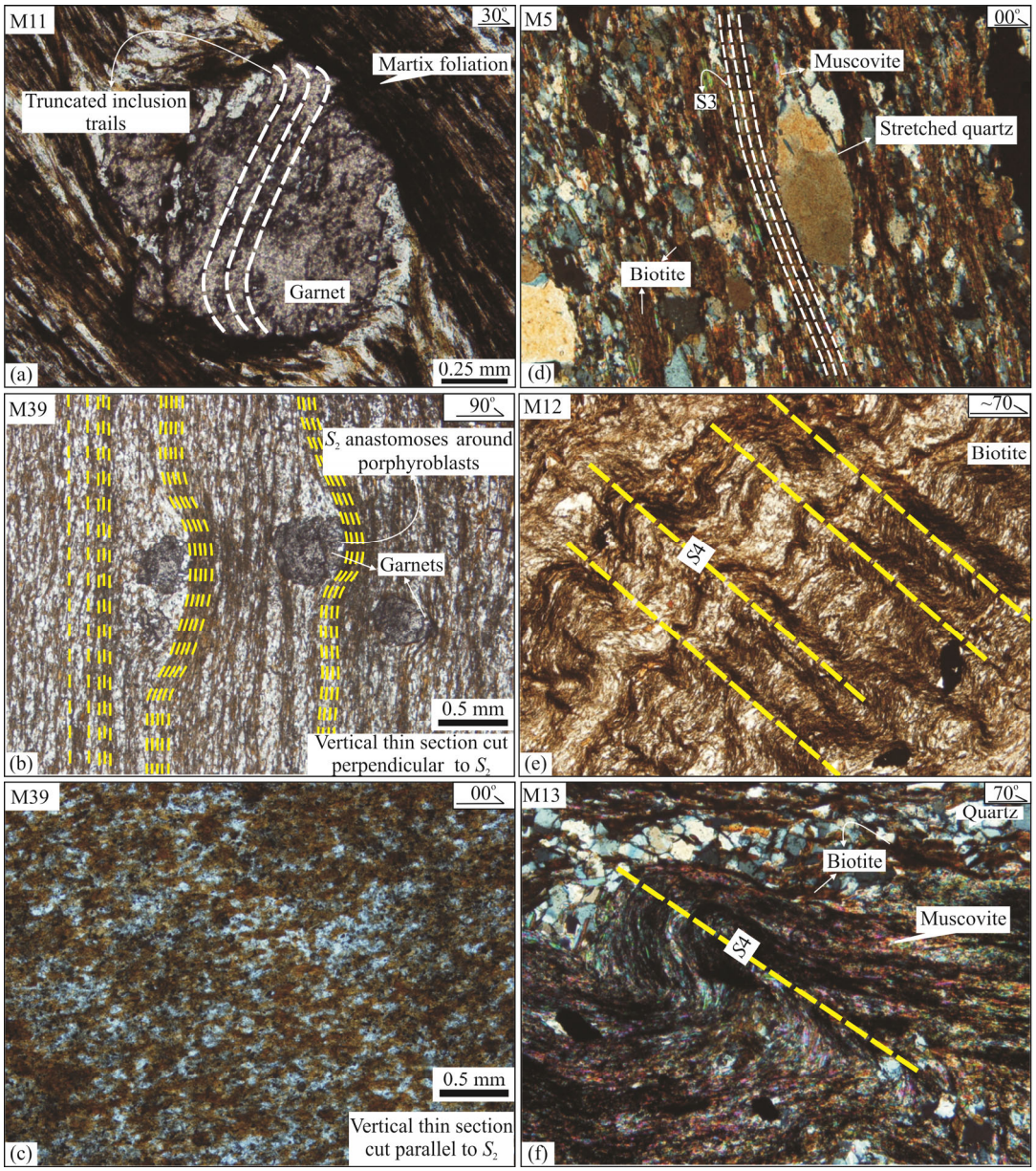

Figure 7. (a) Photomicrograph showing S_1 preserved as inclusion trails in garnet porphyroblast, the inclusions trails are predominantly consist of elongated quartz and are strongly truncated by the matrix foliations. (b), (c) Photomicrographs showing N-S trending S_2 in vertical thin sections cut at 90° and parallel to true north. (d) Photomicrograph illustrating E-W trending S_3 in vertical thin section cut parallel to true north. (e), (f) Photomicrographs showing newly developed S_4 crenulation cleavage in the matrix. These vertical thin sections are cut at 70° to true north. Note the three types of cleavages are very heterogeneously developed across the study area.

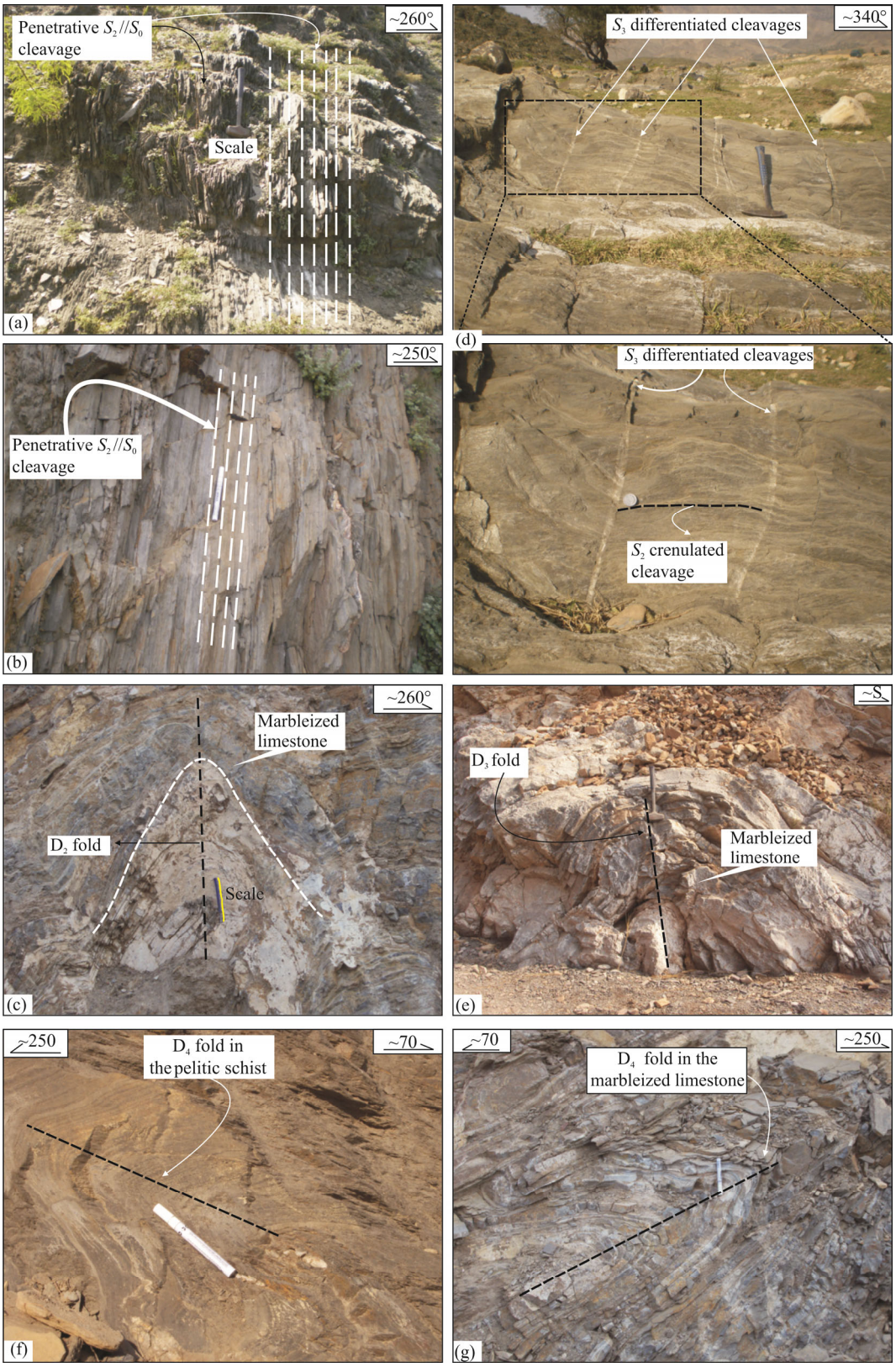

Figure 8. (a), (b) Oriented field photographs showing bedding parallel N-S trending S_2 in the pelitic unit of the Lowara Mena Formation. (c) Tight mesoscopic D_2 fold with N-S trending axial plane in the marbleized unit. Note the same axial plane S_2 foliations are parallel to bedding in the metapelites. (d) Oriented field photograph illustrating steeply dipping S_3, which intersects S_2 in the pelitic unit of the Lowara Mena Formation. Coin diameter is 2.2 cm. (e) Oriented field photograph looking towards east showing D_3 sub-vertical mesoscopic fold in the marbleized limestone unit exposed south of study area. (f), (g) Oriented field photographs showing NNW-SSE trending D_4 related mesoscopic folds in the pelitic and marbleized beds. Marker length is 13.2 cm.

strongly aligned phyllosilicates mineral (muscovite and biotite). Mineral lineation L_2^2 (Fig. 9a) and mesoscopic D_2 fold axes trend ~N-S. The L_3^3 mineral lineation (Figs. 9b, 9c) and mesoscopic D_3 fold axes trend in the range between ~070º to 105º. The D_4 deformation event produced a 330º–340º trending mineral lineation L_4^4 (Figs. 9d, 9e) and mesoscopic D_4 fold axes.

6 MICRO- TO MESOSCOPIC STRUCTURES RELATIONSHIP

Mesoscopic and microscopic structures show a close resemblance to each other at all scales of observation. The S_1 was not observed at outcrop scale. It is mainly preserved as inclusion trails in garnet porphyroblasts, which also define FIA 1 (Figs. 4, 7a). The N-S striking S_2 foliation is moderately to steeply dipping at the outcrop scale. At thin section scale N-S trending S_2 is preserved as differentiated crenulation cleavage seams or M-domains (Figs. 7b, 7c). It wraps around garnet porphyroblasts preserving FIA 1. The ENE-WSW striking S_3 foliation intersects bedding parallel S_2 foliation approximately at a high angle in the metapelitic beds. On a microscopic scale, S_3 crenulation cleavage is subvertical and ENE-WSW trending (Fig. 7d). The S_4 was observed as a shallow dipping axial plane foliation at the outcrop scale. The orientation of S_4 ranges between 330º–340º and is moderately dipping towards the SE. The S_4 at a microscopic scale preserved is in the form of an axial planar foliation and crenulates the matrix foliation (Figs. 7e, 7f).

7 DISCUSSION

7.1 Tectonic Significance of Microscopic to Mesoscopic Structures

Detailed micro- to mesoscopic structural investigations in multiply deformed rocks of the Mula Gori region reveal a more complex deformation history than has previously been established. The interrelationship of microscopic, mesoscopic and macroscopic structural events show four deformation events in the exposed southwestern part of the western hinterland in the Mula Gori region. The D_1, D_2, and D_3 related structures in this part of the western hinterland zone show a remarkable resemblance to the F_1/F_2, F_3, and F_4 related structures described by DiPietro et al. (2008) and Anczkiewicz et al. (1998) in the eastern part of the western hinterland zone. According to DiPieto et al. (2008), F_1/F_2 related fold axes mainly trend in an NW-SE direction. However, the mineral lineations on S_2 are variably oriented in NW-SE, NE-SW and E-W directions. The NE-SW is the dominant trend of the mineral stretching lineations established from granitic gneisses and the Kishora mélange (Anczkiewicz et al., 1998; Fernandez, 1983). The NE-SW trending mineral lineations in the eastern hinterland zone are similar to the trend of FIA 1 in the western hinterland zone. However, we did not observe mesoscopically early NW-SE trending fold axes and mineral stretching lineations in our study area. The NE-SW trending FIA set 1 preserved in garnet porphyroblasts shows NW-SE horizontal bulk shortening. The N-S trending D_2 deformation fabrics, stretching lineations and fold axes indicate E-W shortening. The D_2 produced N-S trending regional anticlines and synclines that fold all thrusts older than Kohistan thrust across the western hinterland zone (cf., Kazmer, 1986). Regionally, the D_2 deformation event correlates with the N-S trending D_3 in the Malakand, Mingora and Beshman regions exposed in the northeastern hinterland zone (cf., DiPietro et al., 2008; Anczkiewicz et al., 1998; Treloar et al., 1989). The ENE-WSW trending FIA 2 in the rim of porphyroblasts containing FIA 1 in the core and in porphyroblasts where the inclusion trails are continuous with the matrix, D_3 folds and L_3^3 mineral stretching lineations indicate NNE-SSW bulk shortening. In this region, the D_3 deformation event is equivalent to the Middle to Late Miocene south directed F_4 deformation event in the northeastern part of the western hinterland zone. This event produced regional

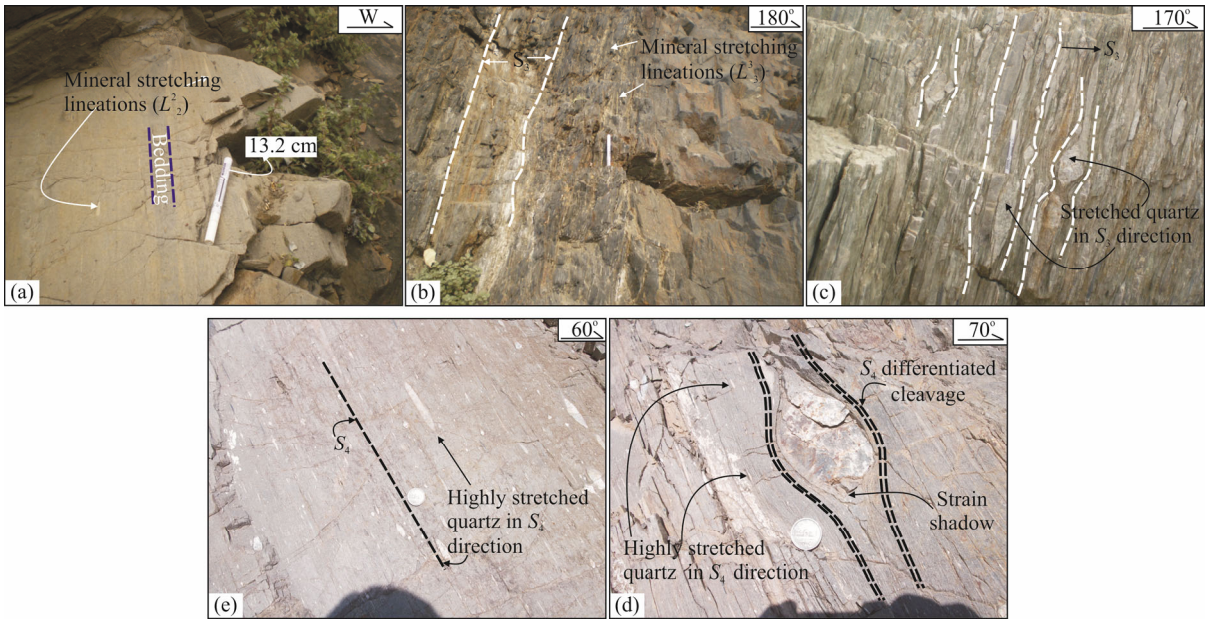

Figure 9. Oriented field photographs showing, (a) mineral lineation (L_2^2) parallel to bedding, (b), (c) mineral lineation (L_3^3) defined by aligned quartz and feldspar grains, L_3^3 mineral lineation trending parallel to D_3 fold axes in the region, (d), (e) mineral lineations (L_4^4) aligned parallel to S_4 foliation in the region. Coin diameter is 2.2 cm and pen length is 13.2 cm.

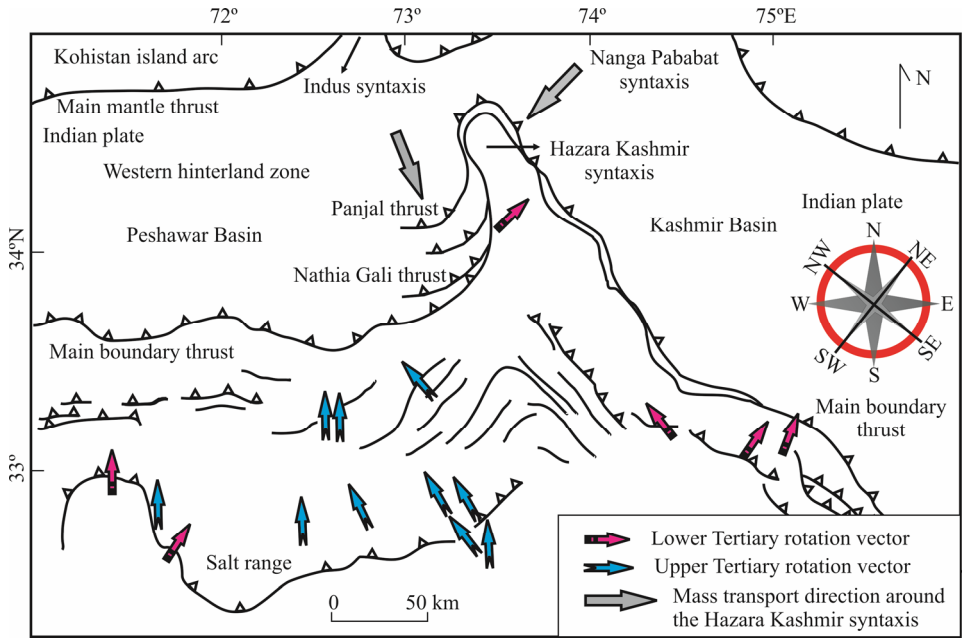

Figure 10. Regional tectonic map showing counterclockwise rotation of the Lower and Upper Tertiary paleomagnetic vector and mass transport direction of the rocks exposed in the west of the HKS (after Bossart et al., 1989).

scale E-W trending structures across the Indian plate. Similarly, the rocks north of the MMT in the Kohistan island arc are also characterized by E-W trending structures (cf., DiPietro and Lawrence, 1991). Metamorphism related with the D_3 deformation event produced garnets that preserve FIA 2 and staurolite porphyroblasts. The NNE-SSW shortening during D_3 produced regional structures that dominate the foreland basin of Pakistan. The D_3 tectonic event accompanied southward thrusting of the Kohistan island arc along the MMT over the northern metamorphosed margin of the Indian plate during the Oligocene (cf., DiPietro and Lawrence, 1991). The E-W trending D_3 structures were subsequently refolded around the NNW-SSE trending fold axis of the Hazara-Kashmir syntaxis (HKS; cf., Pogue et al., 1999; Bossart et al., 1988; Fig. 1a). The regional scale Khairabad-Panjal thrust, the Hissartang-Nathia Gali thrust and the main boundary thrusts are rotated counterclockwise in the apex region of the HKS (Fig. 1a). The HKS tectonic event has not only affected the major faults in the western hinterland zone of Pakistan but has also affected the rocks exposed on its western limb (Bossart et al., 1988). Similarly, the paleomagnetic studies of the Lower and Upper Tertiary molasse sediments on the western side of the HKS in the Potwar Basin, salt range and Attock Cherat range also indicate counterclockwise rotation of these tectonic terrains relative to the Indian craton with respect to the true geographic north (Fig. 10; Bossart et al., 1989; Opdyke et al., 1982). The overprinting shallow dipping NNW-SSE trending D_4 deformation fabrics, L_4^4 mineral stretching lineations and axial plane foliation suggest ENE-WSW bulk horizontal shortening has occurred in the southwestern part of the western hinterland zone. The NW verging asymmetric D_4, which is less pervasively developed in the region, has not been reported micro- to mesoscopically in the northeastern part of the western hinterland zone. It appears that D_4 NNW-SSE fabrics that formed in the western hinterland zone after the Kohistan island arc and Indian plate collision resulted from ENE-WSW bulk shortening related to the HKS tectonic event.

7.2 Metamorphism

Petrographic examination of 50 samples indicates prograde metamorphism. In Fig. 2c, the truncation of inclusion trails in the core, which was then overgrown by garnet in the rim suggests that garnet growth occurred during D_1 and D_3. The grade of metamorphism increases towards the north with the first appearance of staurolite during D_3 in samples M10, M11 and M50 (Fig. 1b). This increase in grade of metamorphism from south to north is remarkably consistent across the western hinterland zone. From the present investigation it is clear that majority of the rock samples corresponds to green schist facies, however the presence of staurolite in these rocks towards north indicates medium amphibolite facies metamorphism in the Mula Gori region. The continuity of inclusion trails preserved in the staurolite porphyroblasts with the matrix indicates that staurolite postdates S_2 and FIA 1 garnet growth across the region.

7.3 Deformation Partitioning

Pressure, temperature, bulk composition and deformation are key factors for the evolution of different metamorphic index mineral assemblages in metamorphic rocks (Zeh and Holness, 2003; Spear, 1993). Deformation partitions in a rock into progressive shearing along differentiated crenulation cleavage and coaxial progressive shortening in the crenulation hinge region occurs at all scales of observations (Bell and Bruce, 2006; Bell et al., 2004). Deformation partitioning at all scales plays significant role in controlling the sites of porphyroblast nucleation in zones of progressive shortening and with phyllosilicates concentrated in differentiated crenulation cleavages (Figs. 11a, 11b). Similarly if the deformation partitioning is such that no crenulation hinges develop at the scale of a porphyroblast, the rocks will not grow porphyroblasts (Bell et al., 2013; Bell and Sanislav, 2011).

At various stages during deformation different minerals take

up different amount of strain depending on mineral type or lithology which results in heterogeneity in rocks when deformation partitioning occurring on a large scale (Bell et al., 2013; Bell, 1985). Due to the large grain size and greater competency relative to the matrix, porphyroblasts normally control the partitioning of deformation around them (Bell et al., 2013; Etheridge and Vernon, 1981). As a result, the ellipsoidal island of matrix similar in width to that of porphyroblast is protected by the effect of progressive shearing around the porphyroblast, which does not cause the rotation of material present within the ellipsoidal island due to the external accommodation of deformation (Bell, 1985). For porphyroblast formation partitioning of deformation is vital, without partitioning of deformation porphyroblast cannot grow (cf., Bell, 1985, 1981). Garnet porphyroblasts containing FIAs 1

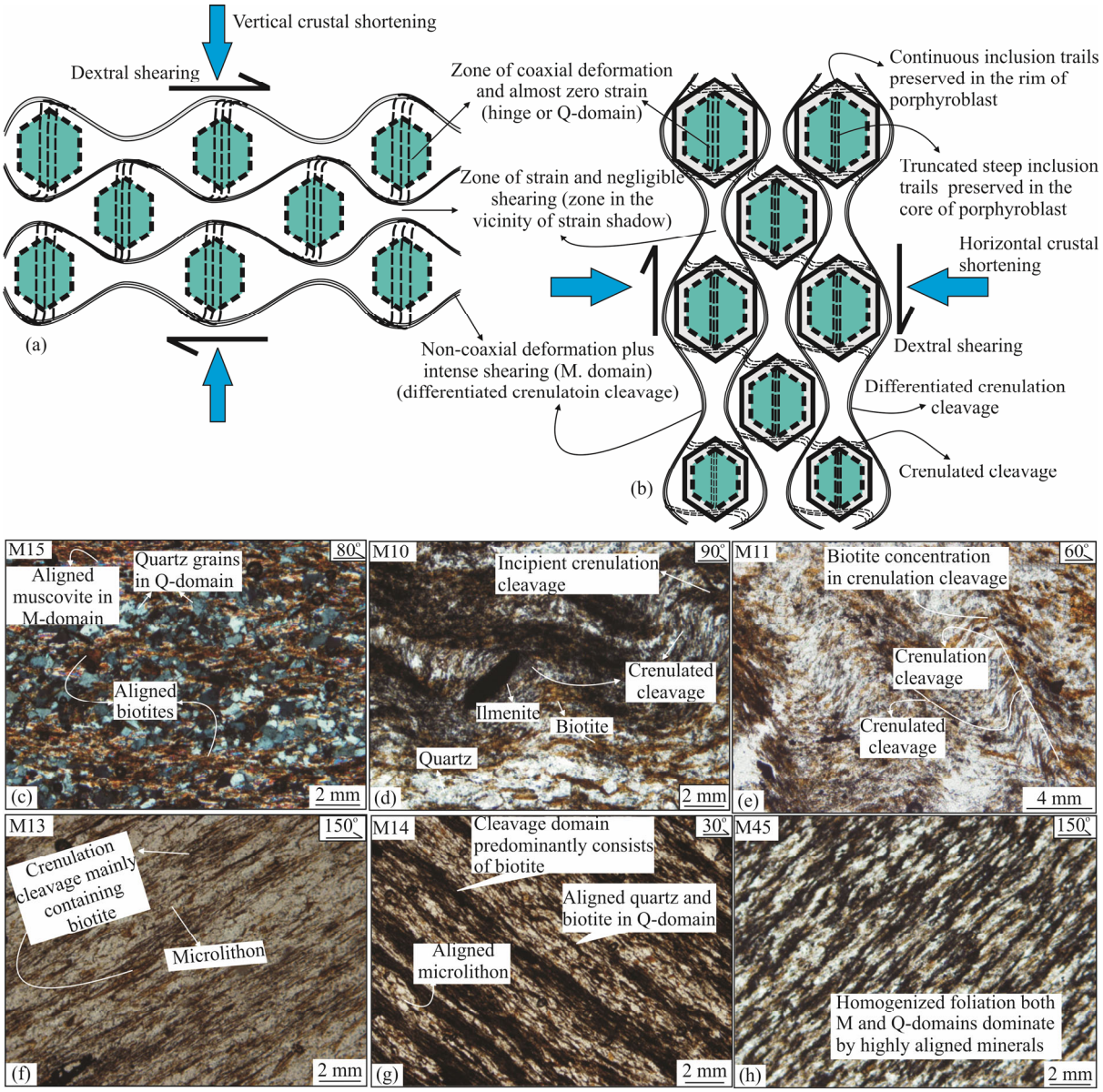

Figure 11. Schematic diagrams showing deformation partitioning at the porphyroblast scale (modified after Bell and Bruce, 2006). (a) Diagram showing vertical crustal shortening that is split into zones of non-coaxial (progressive shearing or differentiated cleavage) and coaxial deformations (progressive shortening or Q-domain). Porphyroblasts, that grew in the vertical crustal shortening preserved steep inclusion trails. Note the inclusion trails, which are preserved in porphyroblasts, are bending clockwise along the differentiated crenulation cleavage. (b) Diagram showing rim growth of porphyroblasts during horizontal crustal shortening. The horizontal inclusion trails preserved in the rim are bending clockwise along the well established differentiated crenulation cleavage in the matrix. Note porphyroblasts did not grow in the zone of shearing. This geometry, which has been established due to deformation partitioning, is vital for porphyroblast growth in any rock. (c) Photomicrograph showing stage 1 of crenulation cleavage development in the matrix. Continuous foliation mainly defined by subparallel micas. (d) Photomicrograph of stage 2 foliation development in the matrix. (e) Photomicrograph showing stage 3 of crenulation cleavage development. (f) Photomicrograph of the matrix foliation preserving stage 4 of crenulation cleavage development. Note the difference in composition and gradual change between the domains. (g) Photomicrograph showing stage 5 of crenulation cleavage development. Note the difference of composition in two domains. (h) Photomicrograph showing stage 6 of crenulation cleavage development. Disjunctive cleavage defined by subvertical biotite rich layers and microlithons. Single barbed arrows show strike and way up.

and 2 predominantly developed in the SE part of the Lowara Mena Formation. The lack of garnet porphyroblasts in the NW portion of the formation (Fig. 1b) shows that the deformations related with FIAs 1 and 2 partitioned such that it did not affect lithologically similar rocks adjacent to the NW when it impacted on the SE part of the formation. The lack of porphyroblast across the NW side of the formation suggests the lack of locally finer scale partitioning of deformation was possibly due to the competent crystalline rocks surrounding the formation (Fig. 1b). Similarly due to deformation heterogeneity all six developmental stages of crenulation cleavage were observed in these rocks (see Bell and Rubenach, 1983 for detail). The six stages of crenulation cleavage were observed in different samples (Figs. 11c–11g), which indicates more localized deformation partitioning at all scale of observation during these periods of bulk shortening across the region.

8 CONCLUSION

The tectono-metamorphic evolution of the Silurian–Devonian rocks exposed in the southwestern part of the western hinterland zone is characterized by a very complex multiple deformational structures, tectonism and metamorphism since the collision of the Indian plate and Kohistan island arc. Resolving succession of overprinting deformational structures and metamorphism in multiply deformed active orogenic belts give a robust constraint on sequential crustal shortening direction and successive metamorphic minerals growth. However, in these belts much of the early tectono-metamorphic history preserved in the form of foliations erased from the matrix due to reuse of the early foliations by the younger ones. This fact does not provide access to understanding extraordinary extent tectonism in the active evolving orogenic belts. In such scenario preservation of the early matrix foliations in the form of inclusion trails in porphyroblasts of different generations preserve a much complex tectonic history. The S_1 related foliations and mesoscopic structures, which are obliterated by the younger deformations in the matrix and at outcrop are preserved in the form of fine grained sigmoidal quartz inclusions in garnet porphyroblasts. The NE-SW trending FIA set 1 in the core of garnet porphyroblasts and in garnets where the inclusion trails are truncated by the matrix indicates NW-SE horizontal bulk shortening. This tectonic event is succeeded by E-W horizontal bulk shortening during D_2, which has been tightly constrained from the well defined S_2 matrix foliations, mesoscopic mineral lineations and outcrop scale D_2 fold axes. The S_2 anastomosed around FIA set 1 garnet porphyroblasts. The FIA set 2 preserved in the second phase garnet porphyroblasts with continuous inclusion trails, S_3 matrix foliations, D_3 fold axes and L_3^3 mineral stretching lineations indicate NNE-SSW horizontal bulk shortening. In this region, D_3 deformation event is equivalent to the Middle to Late Miocene south directed F_4 deformation event in the northeastern part of the western hinterland zone. The tectonic imprints of the HKS in the southwestern part of the western hinterland zone have been observed at micro- to mesoscopic scales. The NW verging less pervasively developed asymmetric D_4, S_4 matrix foliations and L_4^4 mineral stretching lineations related with HKS tectonic event post-dates MMT, Khairabad-Panjal thrust fault, Hissartang thrust fault and MBT. The imprints of the HKS have not been reported at micro- to mesoscopic scales in the northeastern part of the western hinterland zone.

ACKNOWLEDGMENTS

We gratefully acknowledge the National Centre of Excellence in Geology, University of Peshawar for providing funds and logistical support during this research. We thank Dr. Kyle Larson (University of British Columbia, Canada) for his resourceful discussion on tectonics of Pakistan and Himalaya. We are thankful to the anonymous reviewers and the editors, their thoughtful comments and suggestions have fabulously improved the manuscript. The final publication is available at Springer via http://dx.doi.org/10.1007/s12583-016-0717-1.

REFERENCES CITED

Abu Sharib, A. S. A. A., Bell, T. H., 2011. Radical Changes in Bulk Shortening Directions during Orogenesis: Significance for Progressive Development of Regional Folds and Thrusts. *Precambrian Research*, 188(1–4): 1–20

Adshead-Bell, N. S., Bell, T. H., 1999. The Progressive Development of a Macroscopic Upright Fold Pair during Five Near-Orthogonal Foliation-Producing Events: Complex Microstructures versus a Simple Macrostructure. *Tectonophysics*, 306(2): 121–147. doi:10.1016/s0040-1951(99)00055-4

Aerden, D., 2005. Comment on "Reference Frame, Angular Momentum, and Porphyroblast Rotation" by Dazhi Jiang and Paul F. Williams. *Journal of Structural Geology*, 27(6): 1128–1133. doi:10.1016/j.jsg.2005.04.005

Ahmad, M., Ali, K. S. S., Khan, B., et al., 1969. The Geology of the Warsak Area, Peshawar, West Pakistan. *Geological Bulletin University of Peshawar*, 4: 44–78

Ali, A., 2010. The Tectono-Metamorphic Evolution of the Balcooma Metamorphic Group, North-Eastern Australia: A Multidisciplinary Approach. *Journal of Metamorphic Geology*, 28(4): 397–422. doi:10.1111/j.1525-1314.2010.00871.x

Anczkiewicz, R., Burg, J. P., Hussain, S. S., et al., 1998. Stratigraphy and Structure of the Indus Suture in the Lower Swat, Pakistan, NW Himalaya. *Journal of Asian Earth Sciences*, 16(2/3): 225–238

Bell, T. H., 1981. Foliation Development—The Contribution, Geometry and Significance of Progressive, Bulk, Inhomogeneous Shortening. *Tectonophysics*, 75(3/4): 273–296

Bell, T. H., Rubenach, M. J., 1983. Sequential Porphyroblast Growth and Crenulation Cleavage Development during Progressive Deformation. *Tectonophysics*, 92(1–3): 171–194

Bell, T. H., 1985. Deformation Partitioning and Porphyroblast Rotation in Metamorphic Rocks: A Radical Interpretation. *Journal of Metamorphic Geology*, 3: 109–118

Bell, T. H., 1986. Foliation Development and Refraction in Metamorphic Rocks: Reactivation of Earlier Foliations and Decrenulation due to Shifting Patterns of Deformation Partitioning. *Journal of Metamorphic Geology*, 4(4): 421–444

Bell, T. H., Hickey, K. A., 1998. Multiple Deformations with Successive Subvertical and Subhorizontal Axial Planes in the Mount Isa Region: Their Impact on Geometric Development and Significance for Mineralization and Exploration. *Economic Geology*, 93(8): 1369–1389

Bell, T. H., Ham, A. P., Hickey, K. A., 2003. Early Formed Regional Antiforms and Synforms that Fold Younger Matrix Schistosities: Their Effect on Sites of Mineral Growth. *Tectonophysics*, 367(3/4): 253–278

Bell, T. H., Ham, A. P., Kim, H. S., 2004. Partitioning of Deformation along an Orogen and Its Effects on Porphyroblast Growth during Orogenesis. *Journal of Structural Geology*, 26(5): 825–845. doi:10.1016/j.jsg.2003.11.021

Bell, T. H., Bruce, M. D., 2006. The Internal Inclusion Trail Geometries Preserved within a First Phase of Porphyroblast Growth. *Journal of Structural Geology*, 28(2): 236–252. doi:10.1016/j.jsg.2005.11.001

Bell, T. H., Sanislav, I. V., 2011. A Deformation Partitioning Approach to Resolving the Sequence of Fold Events and the Orientations in which They Formed across Multiply Deformed Large-Scale Regions. *Journal of Structural Geology*, 33(7): 1206–1217. doi:10.1016/j.jsg.2011.03.014

Bell, T. H., Sapkota, J., 2012. Episodic Gravitational Collapse and Migration of the Mountain Chain during Orogenic Roll-on in the Himalayas. *Journal of Metamorphic Geology*, 30(7): 651–666. doi:10.1111/j.1525-1314.2012.00992.x

Bell, T. H., Rieuwers, M. T., Cihan, M., et al., 2013. Inter-Relationships between Deformation Partitioning, Metamorphism and Tectonism. *Tectonophysics*, 587: 119–132. doi:10.1016/j.tecto.2012.06.014

Bossart, P., Dietrich, D., Greco, A., et al., 1988. The Tectonic Structure of the Hazara-Kashmir Syntaxis, Southern Himalayas, Pakistan. *Tectonics*, 7(2): 273–297

Bossart, P., Ottiger, R., Heller, F., 1989. Paleomagnetism in the Hazara-Kashmir Syntaxis, NE Pakistan. *Eclogae Geologicae Helvetiae*, 82: 585–601

Cao, H., Fletcher, C., 2012. FIA Trends along the Precambrian Rocky Mountains: A New Approach to Timing Continental Docking. *Journal of Metamorphic Geology*, 30(7): 639–650. doi:10.1111/j.1525-1314.2012.00994.x

Cihan, M., Parsons, A., 2005. The Use of Porphyroblasts to Resolve the History of Macro-Scale Structures: An Example from the Robertson River Metamorphics, North-Eastern Australia. *Journal of Structural Geology*, 27(6): 1027–1045. doi:10.1016/j.jsg.2005.02.004

DiPietro, J. A., Ahmad, I., Hussain, A., 2008. Cenozoic Kinematic History of the Kohistan Fault in the Pakistan Himalaya. *Geological Society of America Bulletin*, 120(11/12): 1428–1440. doi:10.1130/b26204.1

Dipietro, J. A., Lawrence, R. D., 1991. Himalayan Structure and Metamorphism South of the Main Mantle Thrust, Lower Swat, Pakistan. *Journal of Metamorphic Geology*, 9(4): 481–495. doi:10.1111/j.1525-1314.1991.tb00541.x

Etheridge, M. A., Vernon, R. H., 1981. A Deformed Polymictic Conglomerate—The Influence of Grain Size and Composition on the Mechanism and Rate of Deformation. *Tectonophysics*, 79(3/4): 237–254

Fernandez, A., 1983. Strain Analysis of a Typical Granite of the Lesser Himalayan Cordierite Granite Belt: The Mansehra Pluton, Northern Pakistan. In: Shams, F. A., ed., Granites of the Himalayas, Karakoram, and Hindu Kush. Institute of Geology, Punjab University, Lahore. 183–200

Hayward, N., 1990. Determination of Early Fold Axis Orientations in Multiply Deformed Rocks Using Porphyroblast Inclusion Trails. *Tectonophysics*, 179(3/4): 353–369

Hickey, K. A., Bell, T. H., 2001. Resolving Complexities Associated with the Timing of Macroscopic Folds in Multiply Deformed Terrains: The Spring Hill Synform, Vermont. *Geological Society of America Bulletin*, 113(10): 1282–1298

Huston, D. L., 1990. The Stratigraphic and Structural Setting of the Balcooma Volcanogenic Massive Sulphide Lenses, Northern Queensland. *Australian Journal of Earth Sciences*, 37(4): 423–440. doi:10.1080/08120099008727942

Kazmer, C., 1986. The Main Mantle Thrust Zone at Jowan Pass Area: Swat, Pakistan: [Dissertation]. University of Cincinnati, Cincinnati

Kazmi, A. H., Rana, R. A., 1982. Tectonic Map of Pakistan Scale 1: 2 000 000. Geological Survey of Pakistan, Quetta

Khan, A., Aslam, M., Khan, R. N., 1989. Revised Stratigraphy of the Paleozoic Rocks, Khyber Agency, NWFP, Pakistan. *Geological Survey of Pakistan*, 431: 1–11

Opdyke, N. D., Johnson, N. M., Johnson, G. D., et al., 1982. Paleomagnetism of the Middle Siwalik Formations of Northern Pakistan and Rotation of the Salt Range Decollement. *Palaeogeography*, *Palaeoclimatology*, *Palaeoecology*, 37(1): 1–15. doi:10.1016/0031-0182(82)90055-4

Pogue, K. R., Hylland, M. D., Yeats, R. S., et al., 1999. Stratigraphic and Structural Framework of Himalayan Foothills, Northern Pakistan. *Geological Society of America*, *Special Papers*, 328: 257–274. doi:10.1130/0-8137-2328-0.257

Sanislav, I. V., 2010. A Long-Lived Metamorphic History in the Contact Aureole of the Mooselookmeguntic Pluton Revealed by In Situ Dating of Monazite Grains Preserved as Inclusions in Staurolite Porphyroblasts. *Journal of Metamorphic Geology*, 29(2): 251–273

Shah, A. A., 2009. FIAs (Foliation Intersection/Inflection Axes) Preserved in Porphyroblasts, the DNA of Deformation: A Solution to the Puzzle of Deformation and Metamorphism in the Colorado, Rocky Mountains, USA. *Acta Geologica Sinica*: *English Edition*, 83(5): 971–984

Shah, S. M. I., Siddiqi, R. A., Talent, J. A., 1980. Geology of the Eastern Khyber Agency, North West Frontier Province, Pakistan. *Records of the Geological Survey of Pakistan*, 44: 1–30

Spear, F. S., 1993. Metamorphic Phase Equilibria and Pressure Temperature-Time Paths. Mineralogical Society of America, Washington DC. 799

Treloar, P. J., Williams, M. P., Coward, M. P., 1989. Metamorphism and Crustal Stacking in the North Indian Plate, North Pakistan. *Tectonophysics*, 165(1–4): 167–184

Treloar, P. J., Coward, M. P., Chambers, A. F., et al., 1992. Thrust Geometries, Interferences and Rotations in the Northwest Himalaya. In: McClay, K. R., ed., Thrust Tectonics. Chapman and Hall, New York. 325–342

Zeh, A., Holness, M. B., 2003. The Effect of Reaction Overstep on Garnet Microtextures in Metapelitic Rocks of the Ilesha Schist Belt, SW Nigeria. *Journal of Petrology*, 44(6): 967–994. doi:10.1093/petrology/44.6.967